Development and evaluation of a heat storage-based greenhouse dryer

Manas Jyoti Barooah[1,2], Laxmi Narayan Sethi[1], Abhijit Borah[2], Ajita Tiwari[1*], Aradhana Boruah[1]

(1.Assam University, Silchar, Assam, 788011, India;
2. Assam Agricultural University, Jorhat, Assam, 785013 India)

Abstract: In high-humidity conditions of Northeast India, primary processing systems are scarce in all production catchments. The present study is an original experimental study of developing and evaluating an environmentally friendly heat storage-based greenhouse solar bulk drying system for process standardization and value addition of produce. A polyhouse-type heat storage-based greenhouse dryer (GHD) was developed with design standardization of a hemi-cylindrical section of span 10.2 m and radius 2 m of capacity 1000 kg (with racks), flat plate collectors in inlets, an insulated heat storage cement-concrete base, and an improvised forced convection system. Proper dehydration of spices – Turmeric and Ginger, and minor fruits – Elephant apple, Indian Gooseberry, was done in bulk (>500 kg) and in smaller quantities. Under no load test, the system generates hot air ranging from 42.70˚C to 54.32˚C at an ambient temperature of 28.50˚C to 34.60˚C. The primary drying is predominantly natural convection with a calculated air residence time of 36 seconds, supplemented by humidity sensor-induced forced convection. Initial and final moisture content of 640 kg fresh turmeric dried after proper blanching in one batch range from 85% - 89% to below 11%, respectively, at an average solar radiation of 521.46 watt m^{-2}. The thermal efficiency of the dryer is 28.49%.

Keyword: Greenhouse Solar Dryer (GHD), Heat storage base, thermal efficiency, bulk drying, solar radiation

Citation: Barooah, M. J., L. N. Sethi, A. Borah, A. Tiwari, and A. Boruah. 2025. Development and evaluation of a heat storage-based greenhouse dryer. Agricultural Engineering International: CIGR Journal, 27(3):235-252.

1 Introduction

In developing countries, open sun drying methods have been practiced for drying of various food products at domestic, farm, agro-industrial, and community levels (Hii et al., 2006). To obtain proper drying under open sun, citrus fruits and volatile compound-containing spices are to be dried at a temperature range of 45°C to 55°C, which is difficult to maintain. Open sun drying is associated with problems like cloudy days, low solar intensity, high nocturnal humidity, and intermittent or unexpected rains. The quality and safety of dried products are compromised due to open sun drying (Ratti and Majumdar, 1997) because of the sluggish drying process and the potential for product loss caused by birds, rats, insects, and other species. Considering these factors, open sun drying is not widely favored.

To ensure the efficiency of economically viable final agricultural produce, agricultural produce must be preserved to reduce spoiling and enable economic

Received date: 2024-11-13 **Accepted date:** 2025-05-10
***Corresponding author: Ajita Tiwari.** Assam University, Silchar, Assam, India. Email: ajitatiwari@gmail.com.

transportation. Therefore, having well-designed, energy-efficient drying systems is essential. Mechanical drying by electricity or fossil fuel (coal or diesel) is not feasible because of the unstable electric grid supply and the depletion of fossil fuels, respectively. The abundance of sun-radiant energy is the most attractive drying method for developing nations facing an energy crisis. However, because solar energy is sporadic and unavailable at night, its employment is restricted during daylight hours

In general, greenhouse dryers are tunnel dryers and are classified as direct drying systems. Heat storage material combined with phase change material (PCM) has been used by several researchers in greenhouse drying systems. The increase in indoor air temperature was analyzed to be between 6°C and 12°C with a 4 cm thick PCM on the north wall as a thermal storage (Berroug et al., 2011).

A study applied a reflective mirror on the north side of the dryer (Ahmad et al., 2023). It used a 10 mm-thick polystyrene sheet as insulation to maximize solar radiation utilization and minimize heat loss from the north wall. One experimental greenhouse dryer tested with a natural convection process compared performance with concrete, rock-bed, and sand as heat storage materials (Ayyappan et al., 2015). Coconuts dried from 52% to 7% on a wet basis in 78 hours using concrete (time reduced by 55% compared to open sun), sand as a heat-storing material took 66 hours and lowered drying time by 62%, and with rock-bed material, it took 53 hours and drying time was 69% faster. Thermal storage material improved drying efficiency by 11.6%, 11%, and 9.5% for rock-bed, sand, and concrete. Ahmad and Prakash (2020) tested a greenhouse dryer with gravel, black-painted gravel, ground, and concrete floor as heat storage beds. Out of these, the black-painted gravel bed reached 64.4°C, a heat gain of 53% compared to the surroundings.

The present experimental study aims to develop a greenhouse dryer primarily under natural convection mode during the active drying day period. The novelty of this work is in the standardization of symmetrical hemi-cylindrical section specified by radius and span (length), black-coloured, polystyrene insulated cement-concrete base, and automatic switching between natural and forced convection modes improves the efficiency and functional capabilities of the dryer

A comprehensive greenhouse solar drier with a designed number of air inlets and outlets is developed for efficient bulk (1000 kg) drying under high-humidity climatic conditions. The loaded dryer was tested at the project site between January and March with relative humidity and temperature in the range from 55% to 99% and 24°C to 32°C, respectively.

Effective greenhouse dryers have the potential to support the preservation of the quality and nutritional value of agricultural products like spices, minor fruits. The results of this study have the potential to be advantageous for different stakeholders, such as farmers, farmer-producing companies, and policymakers. This research can provide valuable insights to enhance drying processes, minimize energy usage, and enhance the overall quality of dried crops, resulting in low-cost dryers with environmental advantages.

2 Methods and materials

2.1 Location of experimental site

The latitude and longitude of the location site are 26.717397, 94.193196, respectively, and the address is ICR Farm, Assam Agricultural University, Borbheta, Jorhat, Assam 785013, India. Typical climatic conditions of the site are such that it has high relative humidity almost throughout the year. June to Sept are the wettest months, and January to March are the driest part of the year (Dikshit and Dikshit, 2014). Figure 1 shows the temperature and relative humidity of a normal non-rainy day in a 24-hour cycle. In this site, there is a considerable drop in ambient relative humidity during day hours, corresponding to higher temperatures, thereby making it an ideal space for drying time. Figure 2 depicts that even in the driest part of the year, there is high relative humidity at nightfall and continues till morning.

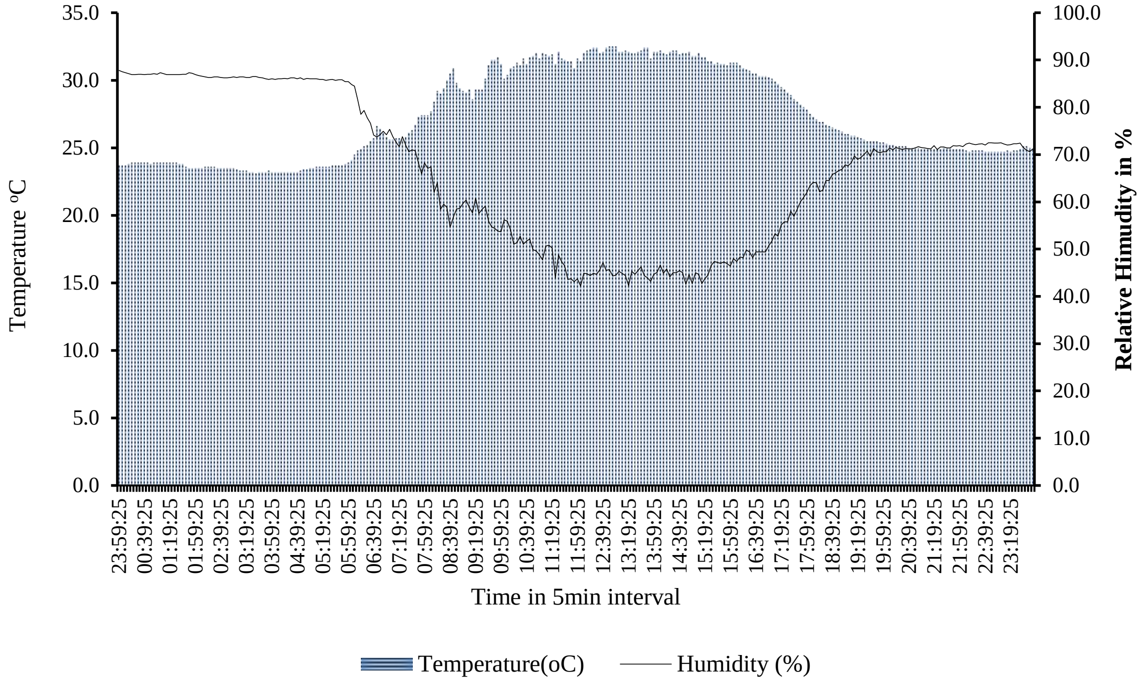

Figure 1 Temperature and humidity variation in 24-hour cycle on a clear day in Summer

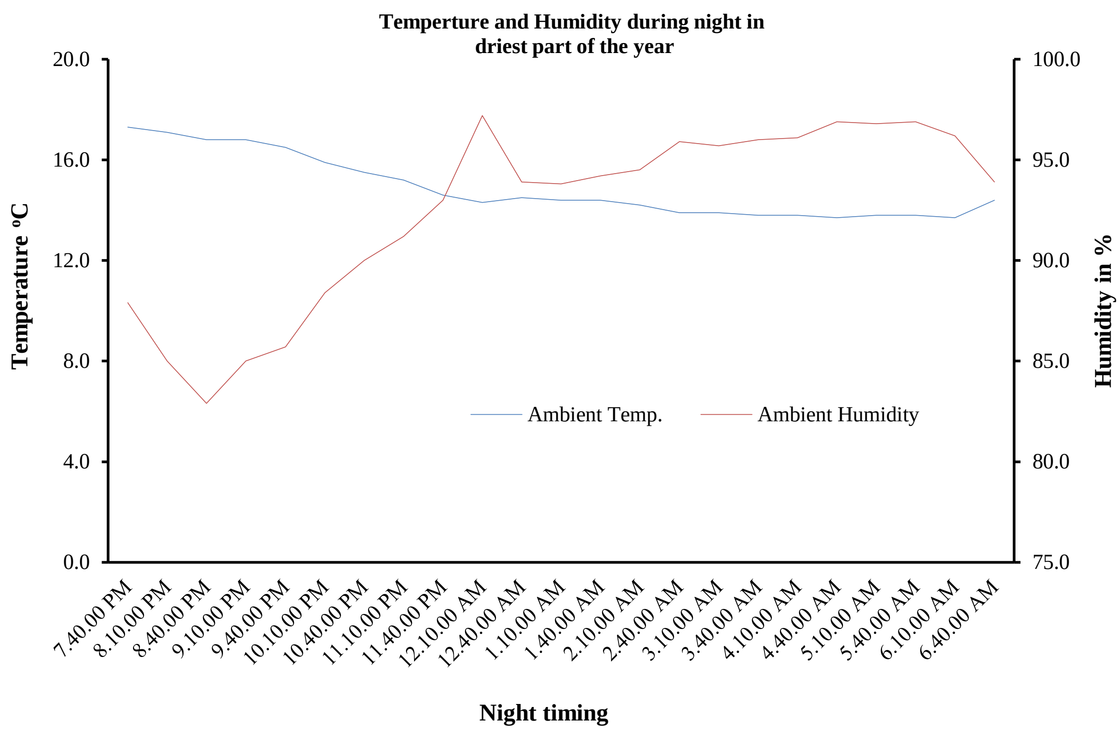

Figure 2 Temperature and Relative humidity, at dark hours in the driest part of the year

In cloudy months like June, average solar radiation can be as low as 50 W m^{-2}. Typical solar radiation during a sunny day in June at the project site is shown in Figure 3. Two-day average solar radiation in June is shown in Figure 4.

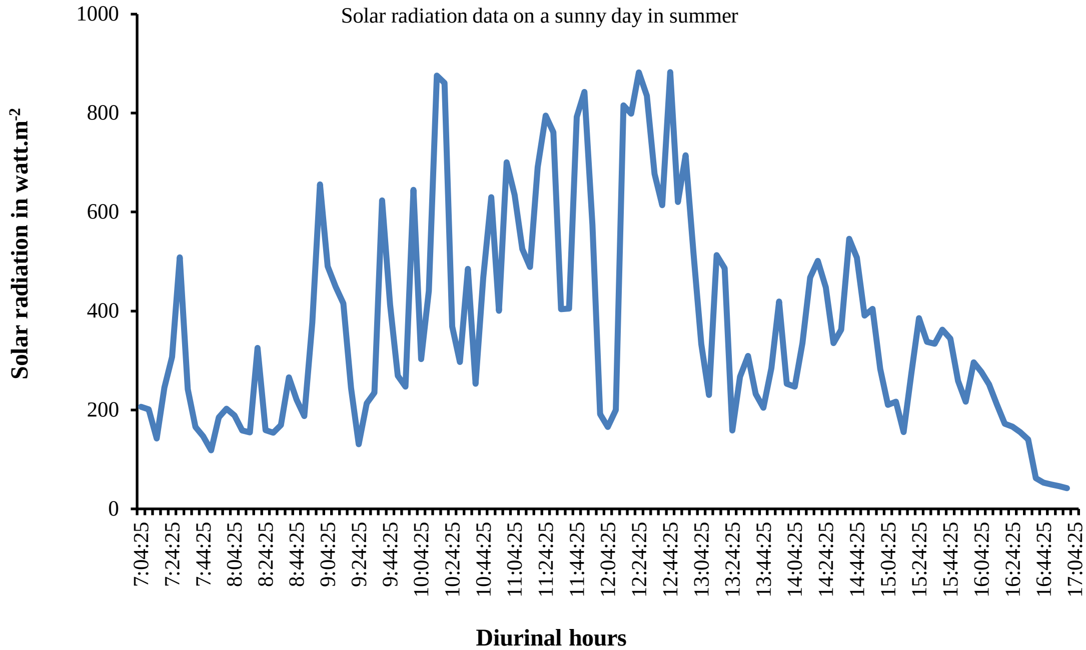

Figure 3 Average solar radiation in a sunny day in June

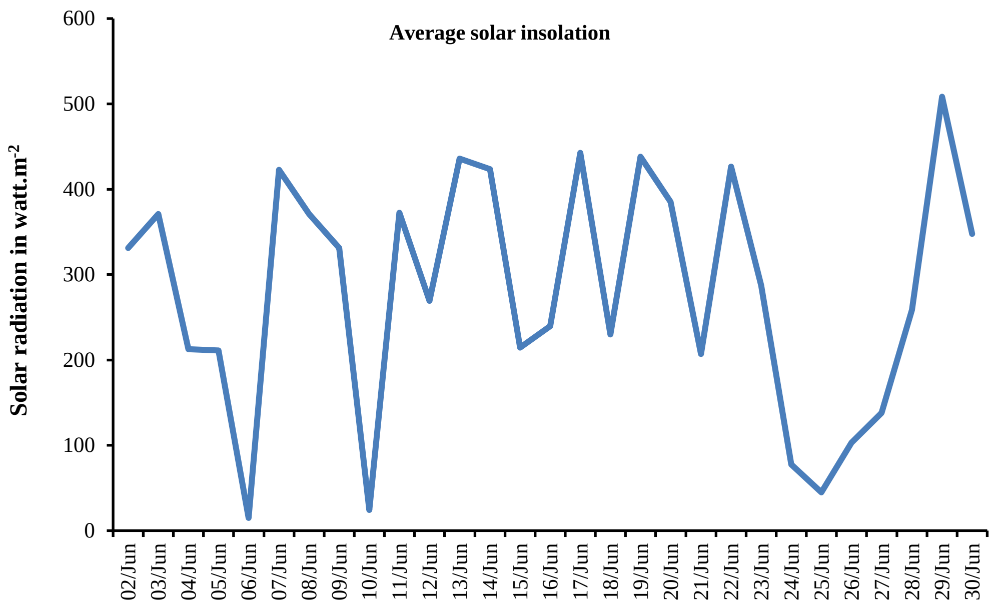

Figure 4 Two-day average Solar radiation

2.2 Incident thermal energy to be used for drying

Based on the classification of dryers proposed by Ekechukwu and Norton (1997), the dryer under discussion is classified as an integral-type passive/active dryer. In integral-type dryers, items are enclosed within transparent walls that facilitate the transmission of insolation, generating natural circulation or natural convection for drying.

The dryer captures solar radiation through the greenhouse effect, resulting in the concentration of solar thermal energy and an increase in the temperature of the air and the cement-concrete (C-C) base structure. Superior volumetric heat capacity of concrete, at 2.086 kJ m^{-3} K^{-1}, compared to 0.001 kJ m^{-3} K^{-1} for air (Engineering toolbox, n.d.), allows the Cement-Concrete base to provide heat for the drying process consistently.

Mathematically, heat gained by a base collector from solar radiation can also be expressed as H_a, (Geankoplis, 2016).

$$H_a = I_c \times A_c \times \eta_c \quad (1)$$

Where, H_a is the heat gained by a base collector from solar radiation (Watts (W), I_c is the solar intensity (W m^{-2}) A_c is the area of heat collector (m^2), and η_c is the collector efficiency(%).

Total heat required, S for drying, can be calculated as -

$$S = S_1 + S_2 + S_3$$

$$S = m_p \times C_p \times (T_p - T_i) + m_w \times C_w \times (T_w - T_i) + m_w \times L \quad (2)$$

Where, S is the total heat, S_1 is the sensible heat of product (kJ), S_2 is Sensible heat of water (kJ), S_3 is Latent heat of water (kJ), m_p is the mass of dry matter of product (kg), Cp is the specific heat of product (kJ kg^{-1} $^{\circ}C^{-1}$), Tp is the final temperature of the product (°C), and T_i is the initial temperature of the product (°C).

1) Sensible heat of the product can be obtained as:

$$S_1 = m_p \times C_p \times (T_p - T_i) \quad (3)$$

2) Sensible heat of water in the product is calculated as:

$$S_2 = m_w \times C_w \times (T_w - T_i) \quad (4)$$

Where, S_2= sensible heat of water, kJ; m_w =initial water content, kg; C_w= specific heat of water, kJ kg^{-1} $^{\circ}C^{-1}$; T_w = final temperature of water, °C; and T_i = initial temperature of product, °C.

3) Latent heat of water is calculated as:

$$S_3 = m_w \times L \quad (5)$$

Where, S_3 = the latent heat of product, kJ; m_w = the quantity of water to be removed, kg; and L = the latent heat of water, KJ kg^{-1}.

4) The thermal efficiency of the solar tunnel drier was estimated using Equation (Ayyappan and Mayilsamy, 2012),

$$\eta_{th} = \frac{m_{w'} \times hfg}{A \times I} \quad (6)$$

where, η_{th} = drier thermal efficiency; m_w = the mass of water evaporated in time t { $m_w = (m_i - m_f)$ kg}; hfg = the latent heat of vaporization of water , kJ kg^{-1}; A = the area of the solar tunnel drier , m^2; and I = solar intensity, W m^{-2}.

5) Drying kinetics

In the thin layer drying experiment of turmeric in the greenhouse dryer (GHD), the moisture ratio (MR) of turmeric slices was calculated using the formula –

$$MR = \frac{M - M_e}{M_o - M_e} \quad (7)$$

Where, M = moisture content % (w b) of turmeric at time t; M_e = equivalent moisture content % (w b) of turmeric; M_o = initial moisture content of the material % (w b).

Effective moisture diffusivity

The equation for drying agricultural products like turmeric and ginger in a thin slab may be written as

$$MR = \frac{8}{\pi^2} exp \frac{D_{eff}}{4h^2} \quad (8)$$

The turmeric drying practical is long, taking $n=0$ (Geankoplis, 2016), the equation can be written as

$$A = \frac{8}{\pi^2} \text{ for slab thickness, K}$$

Putting in linear form

$$ln\ (MR) = ln\ A - kt \quad (9)$$

Upon reviewing the literature, most greenhouse dryers had segmented dimensions, such as length × breadth × height (Ayyappan and Mayilsamy, 2012; Seveda, 2012; Rathore and Panwar, 2010). The calculated dimension of the hemi-cylindrical structure in this research is a span of 10.2 m and a diameter of 4 m. Advantages of the hemi-cylindrical shape in comparison to the segmented structure are as follows:

1. Aesthetic-looking structure.
2. Moss growing in the cladding material is reduced.

As shown in Figure 5, the drying inside the dryer is primarily a natural convection process. Convection occurring naturally within a closed space, also known as internal convection, is a crucial phenomenon with substantial practical implications. In energy-related applications, natural convection is the primary mechanism for transporting energy. It is crucial to build enclosures according to this principle to optimize the heat transfer rate.

The cement concrete floor structure acts as a heat storage device, as shown in Figure 6. So even if there is a brief intermittent cloudy period during the day, it does not affect the dryer's functioning because of the heat supply from storage. This platform also acts as a buffer stock of thermal energy. This stored and backed-up solar thermal energy is optimally used for drying purposes.

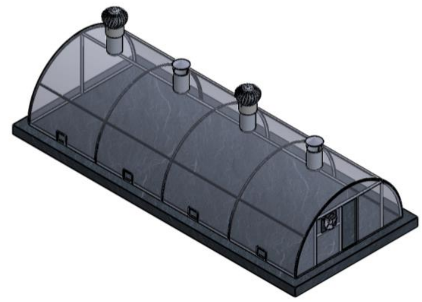

Figure 5 Walk-through type solar tunnel dryer with Cement-concrete base, transparent top, air inlets, hot air outlets, and provision of forced convection

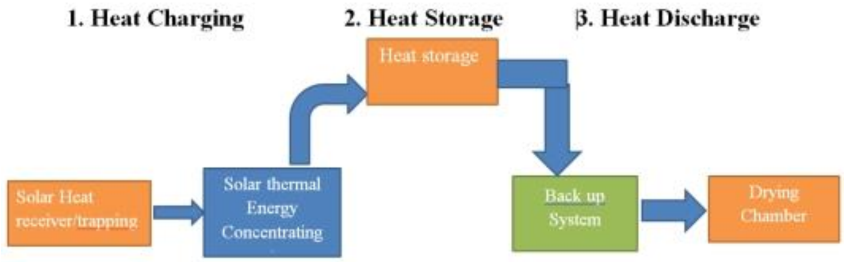

Figure 6 Thermal energy flow chart in greenhouse dryer

The designed hemi-cylindrical shaped structure ensures a natural convection process within the enclosure with the hot surface at the bottom (cement-concrete base) and an adiabatic semicircular shaped upper structure. The adiabatic semicircular structure also acts as a one-way gate for solar thermal radiation.

2.3 Features of GHD for drying

2.3.1 Instrumentation

The following parameters were measured for thermal analysis of the Greenhouse dryer under no load and loaded conditions:

Solar radiation (W m^{-2}) by Pyranometre with logger;

Temperature (°C) sensor-based device with logger;

Relative humidity (%) sensor-based device with logger;

Air flow measurement (m sec^{-1}) by vane type anemometer;

Moisture content measurement of spices and fruits in the loaded condition.

Throughout the experiment, data on solar radiation and the amount of thermal energy available in watts per square meter were analyzed using a digital data logger and a Delta SPN1 Sunshine Pyranometer (LP PYRA 03).

The relative humidity and temperature of the air at various points within and outside the dryer is measured with the help of data loggers. The incoming and exit air velocity at different inlet windows and outlet chimneys was measured by using vane anemometers, respectively. The incoming and outgoing air velocity is 0.4 m sec^{-1} at the start of the day and goes up to 0.9 m sec^{-1}. In addition, the volume of inflow and outflow in m^3 sec^{-1} and the instantaneous temperature and humidity of incoming and outgoing flow were also monitored. Moisture content measurement of drying produce is measured with the help of the Contech Moisture analyzer.

Every day, data on solar radiation was gathered at intervals of 15 to 30 minutes to determine the amount of energy that the sun might provide in watts per square meter. Analysis was also done on how clouds, rain, wind, and daylight hours affect the ability to capture solar thermal energy using instrumentation- Delta SPN1 Sunshine Pyranometer (LP PYRA 03) and digital datalogger. Temperature (°C) and humidity (%) were recorded at a 15 - 30 min time interval with the logger, using the TESTO 175 H1 (Temperature and humidity data logger). Wind flow is measured in m sec^{-1} by a vane-type anemometer used in instrumentation - Testo 410-2.

2.3.2 Parameters assumed

The following features were designed: Number of fresh air inlets and hot air outlets (chimney) based on air residence time to start the natural convection process. Assumed parameters are that the quantity of material to be dried ranges from 650 kg to 1000 kg, from an initial average moisture content (m.c) of 85%-88% (wb) to a final m.c of 10%-11% (wb). Drying is to be accomplished at a temperature range of below 60°C.

2.3.2.1 Air residence time

Air residence time of the greenhouse dryer was calculated, the assumptions were as follows:

Volume of the dryer (V):

$$V = \frac{\pi r^2 h}{2} \quad (10)$$

Where, r = radius of the half tunnel (m), and h = span of the dryer (m).

Area of square inlet opening (A_i):

$A_i = l^2$

Where l = length of the tunnel

Area of the outlet chimney (A_o):

$A_o = \pi r_c^2$

Where r_c = Critical radius of chimney outlet

Volumetric flow rate of the air inlet (Q_i):

$Q_i = A_i v_i$

Time taken to fill the drying chamber (T_f):

$$T_f = \frac{\pi\, r2\, h}{2Ai\ vi}$$

Volumetric flow rate of the air outlet (Q_o):

$Q_o = A_o v_o$

Time taken to empty the drying chamber (T_e):

$$T_e = \frac{\pi\, r^2\, h}{2A_o\, v_o}$$

Hence, residence time

$$Rt = \frac{1}{2} \left[\frac{\pi\, r^2\, h}{A_O v_0 - A_i v_i}\right]$$

Calculating, volumetric space of the Hemi-cylindrical dryer of 2 m Diameter and span of 10.2 m.

$V = \{(\pi \times r^2) \times span\} \times 1/2 = 32.038 / 2 = 16.019$ m^3.

Now assuming 4 number of square inlets of size 20 cm × 20 cm.

Air inlet area (Ai):

$A_i = (0.2 \times 0.2) \times 4 = 0.160$ $m^3\ sec^{-1}$

Now, the recorded air velocity at the inlet (Vi) = 0.4 m sec^{-1}.

Volume of air moving in

$A_i \times V_i = (0.160 \times 0.4)$ $m^3\ sec^{-1} = 0.064\ m^3\ sec^{-1}$

Time required to fill up the dryer $Ti = V / (A_i \times V_i\ A_i \times Vi)$

Hence T_i = 16.019 /0.064 = 250 sec

Similarly, for air moving out through 3-round chimneys of diameter 20cm through natural draft

Air outlet area (Ao) = $\{(3.141 \times 0.04)/4\} \times 3$ = 0.094 m^2

Recorded air velocity at outlet (Vo) = 0.6 m sec^{-1}

Hence, $Ao\ Vo$ = 0.056 $m^3\ sec^{-1}$

Time required to empty the dryer $To = V / Ao\ Vo$

Hence, To = 16.019 / 0.056 = 286 sec

Hence the air residence time during Natural Convection, considering all other factors as constant Rt = 36 sec.

2.4 Thermal energy storage (TES) in the cement-concrete (C-C) base

The TES module consists of a cement-concrete base of the dryer as the heat storage medium for the incident infrared radiation. Reducing heat loss with requisite insulation and reducing moisture creeping up are considered.

2.4.1 Damp proof /powder mixed with cement-concrete mortar

The damp proof powder composition, consisting of aluminosilicate @30-40 wt%, was mixed with cement-concrete mortar.

2.4.2 PVC sheet lying below cement-concrete base at ground level

A moisture barrier for a concrete slab at ground can be made of polyethylene sheeting, epoxy sealer, or concrete moisture sealers. The International Residential Codes (IRC) recommends a minimum 0.25 mm vapor barrier for residential buildings, and the American Concrete Institute (ACI) recommends a minimum of 0.25 mm polyethylene or thicker (ACI committee 302, 2004). Thicker poly is more puncture resistant and provides a better barrier.

During the construction of the cement-concrete base, 30cm high from the ground surface, a 200-micron LDPE sheet layer is provided. The main goal of this LDPE sheet is to form a barrier against the creeping up of soil moisture on the floor during rain. The laying of the plastic sheet is shown in Figure 7. The uppermost floor of the base was made of cement concrete. In this floor construction, damp proof powder is mixed with cement, 250 g per bag of cement (50 kg).

Figure 7 LDPE sheet layering work in cement concrete base construction

The cement-concrete basement was painted with thick black floor paint for better absorption of solar radiation. As seen in Figure 8, this black color was applied to the basement's vertical side that faces magnetic South and West. The absorber base has been covered with a 200-micron UV stabilized cladding material (Suncool – 3201(super)) designed to comply with IS 15287: 2019 standards. The cladding material allows for 30% sunlight diffusion. As seen in Figure 9, polystyrene is used as insulation on the basement's north and east vertical sides to stop heat loss. In addition, the northern cladding wall of the dryer doesn't receive incident solar radiation; as such, this wall is the most vulnerable point of heat loss. On this side of the cladding wall, polystyrene is pasted from inside to a height of 0.45 m from the base.

Figure 8 View of basement and piped structure

Figure 9 Polystyrene pasted for thermal insulation

2.4.3 Cost-effective automation

Under natural convection, four fresh square-shaped air inlet windows of 0.20 × 0.20 m are made near the bottom of the solar tunnel dryer facing the Earth's magnetic south. Three chimneys with a diameter of 0.20 m in the top center line are placed equidistantly positioned in-between the air inlets. This type of solar dryer is being classified under the natural convection type (Ekechukwu and Norton., 1999).

To increase hot air circulation and put the system under forced convection mode, the eastern wall of the dryer has a 58-watt exhaust fan installed with a 1200 m^3

h^{-1} air flow capability based on air residence time, as shown in Figure 10. The fan is automatically turned "on" and "off" with air humidity sensors for forced convection synchronization as shown in Figure 11.

Figure 10 Exhaust fan with cover

Figure 11 Humidity sensor and fan in operation

Flat bed collectors were attached to the magnetic south during daytime to reduce the moisture content of the incoming air. Glass top corrugated flat beds insulated by sawdust from the bottom and boards from two sides were rigidly connected to the solar dryer air inlet openings as shown in Figure 12.

3 Results and discussion

3.1 Physico-thermal properties of ambient air under open sun-drying and target crops

In the present study, the solar thermal load demand is assessed concerning the physical and thermal characteristics of the surrounding air during open sun-drying for drying spices and small fruits. Among the items chosen for drying, ginger is the most crucial due to its fibrous composition. In assessing the specific energy consumption of ginger during open solar drying, the following related parameters were noted.

Average ambient Temperature during day} = 31.3°C

Average ambient Humidity} = 72%

Average intensity of solar radiation during experimental period} - 345.232 watt m^{-2}

Moisture evaporated - 4.3 kg [Initial wt. 5.8 kg, final wt. 1.5 kg]}

Specific energy consumption = 1.866 kW per kg of ginger.

So, for drying 1 kg of produce (spice or minor fruit), one needs 1.866 kW of thermal power,

So, for drying 1 kg of produce (spice or minor fruit), one needs 1.866 kW of thermal power; this is the designed power rating based on which design calculations are calculated. This much energy needs to be delivered to attain the equivalent moisture of the product.

3.1.1 Development of the greenhouse dryer

Based on the assumptions and design calculations, the following different dimensions of the dryer are finalized as shown in Table 1. The designed hemi-cylindrical shaped structure ensures a natural convection process within the enclosure with the hot surface at the bottom (brick concrete base) and an adiabatic semicircular shaped upper structure. The adiabatic semicircular structure also acts as a one-way gate of the solar thermal component, similar to the discussion, which is in line with earlier reported findings (Das et al., 2016). With four air inlets and three air outlets (chimney), the air residence time inside the dryer is calculated to be 36 sec.

Figure 12 Air inlets fitted with flat bed collector

Table 1 Dimensions and design components of the greenhouse solar dryer (GHD)

Components	Specifications
Length of solar tunnel dryer	10.2 m
Diameter of solar tunnel dryer	4 m
Floor area of solar tunnel dryer	40.54 m^2
Area within the drying chamber	34.98 m^2
Height of the dryer at the centre	2 m
Height of the northern insulated wall	0.6 m
Number of chimneys	3
Diameter of the chimney	0.20 m
Height of the chimney	0.75 m
Number of windows	4
Size of window	0.2 X 0.2 m
Total tray area (Each Rack)	2 x 3 m
Number of racks	3
Door size	1.6 x 0.5 m
Exhaust fan capacity	58 Watt

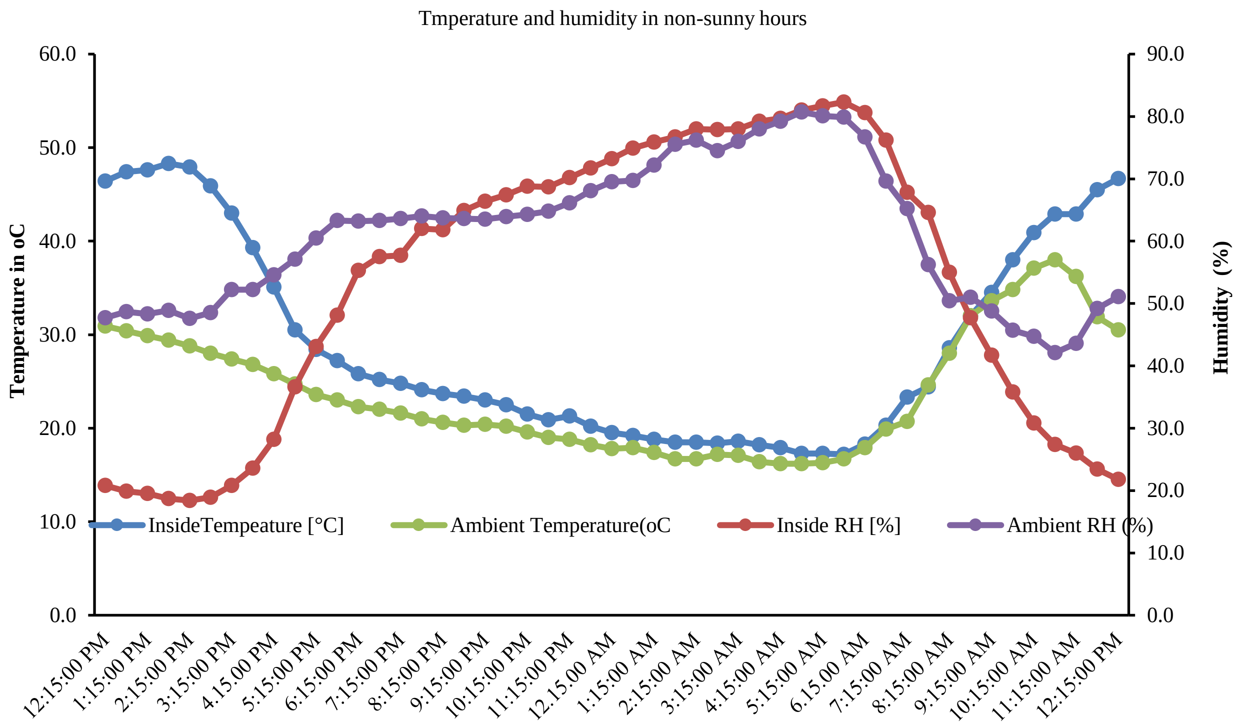

Figure 13 Average temperatures and relative humidity inside the dryer as compared to ambient on a 24-hour cycle under no load condition

3.2 Testing GHD under no-load test

3.2.1 Parameters under no-load test

The design of the solar collector and solar radiation trapping mechanism affects changes in the drying air conditions, including humidity, temperature, and drying time. In a no-load test against solar radiation levels between 478 and 530 W m^{-2}, the drying air temperature peaked between 11:00 AM and 2:00 PM, while the system's relative humidity reached its lowest levels during the same period, as illustrated in Figure 13. The drying air temperature within the greenhouse dryer exceeds that of the external environment by 9°C-18°C on typical sunny days and by 4-10 ° C on partially overcast days during active drying periods.

The temperature inside the dryer is measured at different heights from the base of the dryer. The heat transfer inside the dryer during the daytime is initiated with natural convection mode. The cement-concrete base absorber radiates heat inside the dryer. Fresh ambient air entering from the window maintains the continuity of the convection process. Temperature measured at 60cm (Lower), 120cm (Middle), and 180cm (Upper) from the heat storage base floor is shown in the graph in Figure 14. Different layers of heated air are distinctly recordable from 7 AM to 5 PM. This happens because the air touching the dryer base gets warmer and lighter, moving toward the chimney. On the other hand, low-temperature air from the inlet windows moves in near the base, as shown in Figure 15. The temperature profiles from the cement-concrete base of the Greenhouse solar dryer in the experiment match with the findings reported (Gholamalizadeh and Kim, 2014) about the greenhouse effect in solar chimneys, as well as those in their analysis of flow through the solar dryer duct (Ambesange and Kusekar, 2017).

The marginal reduction of temperature of heated air layers corresponds to a significant decrease in solar radiation (watt m^{-2}) in the afternoon hours, as shown in Figure 16. This is due to the release of thermal energy absorbed by the Cement-concrete base during periods of high solar radiation and the release of heat when solar radiation lowers.

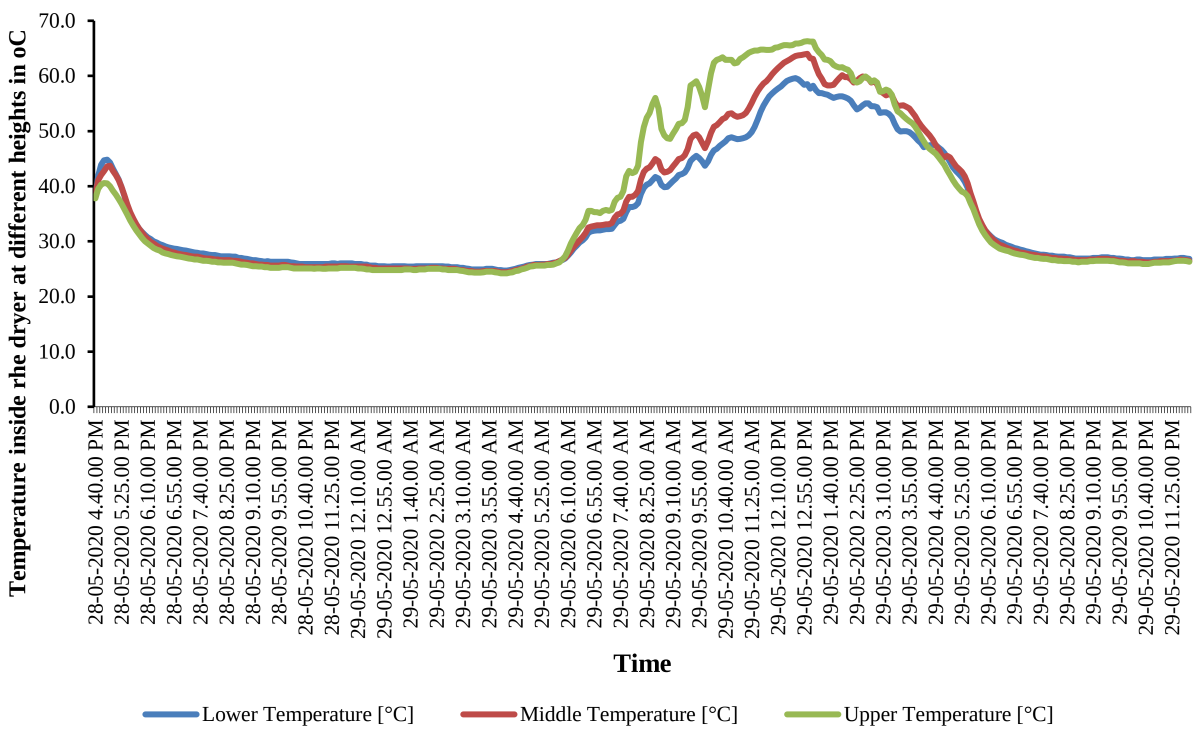

Figure 14 Temperature profile study inside the dryer for 24 hours cycle under Natural Convection

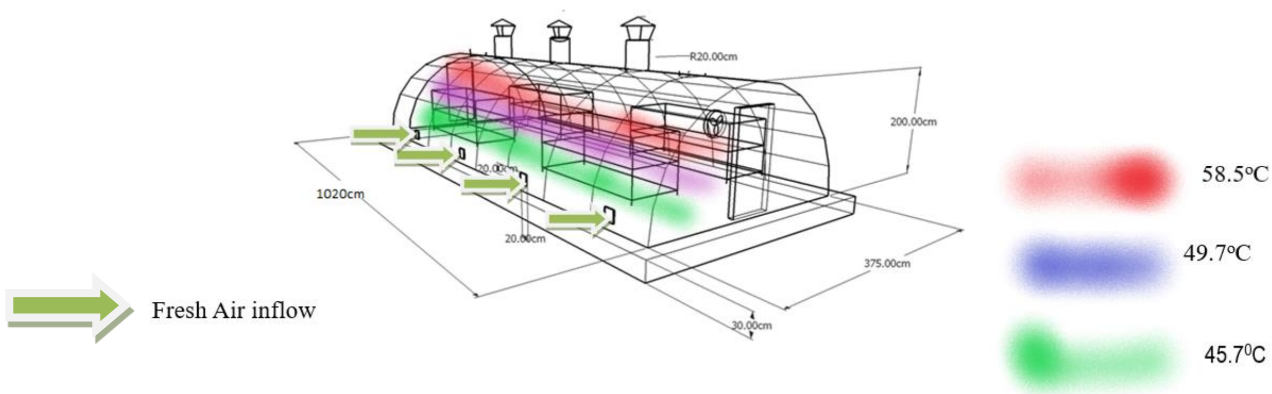

Figure 15 Pictorial view of temperature profile inside GHD at 10.15 AM on 29-5-2021 under no load condition

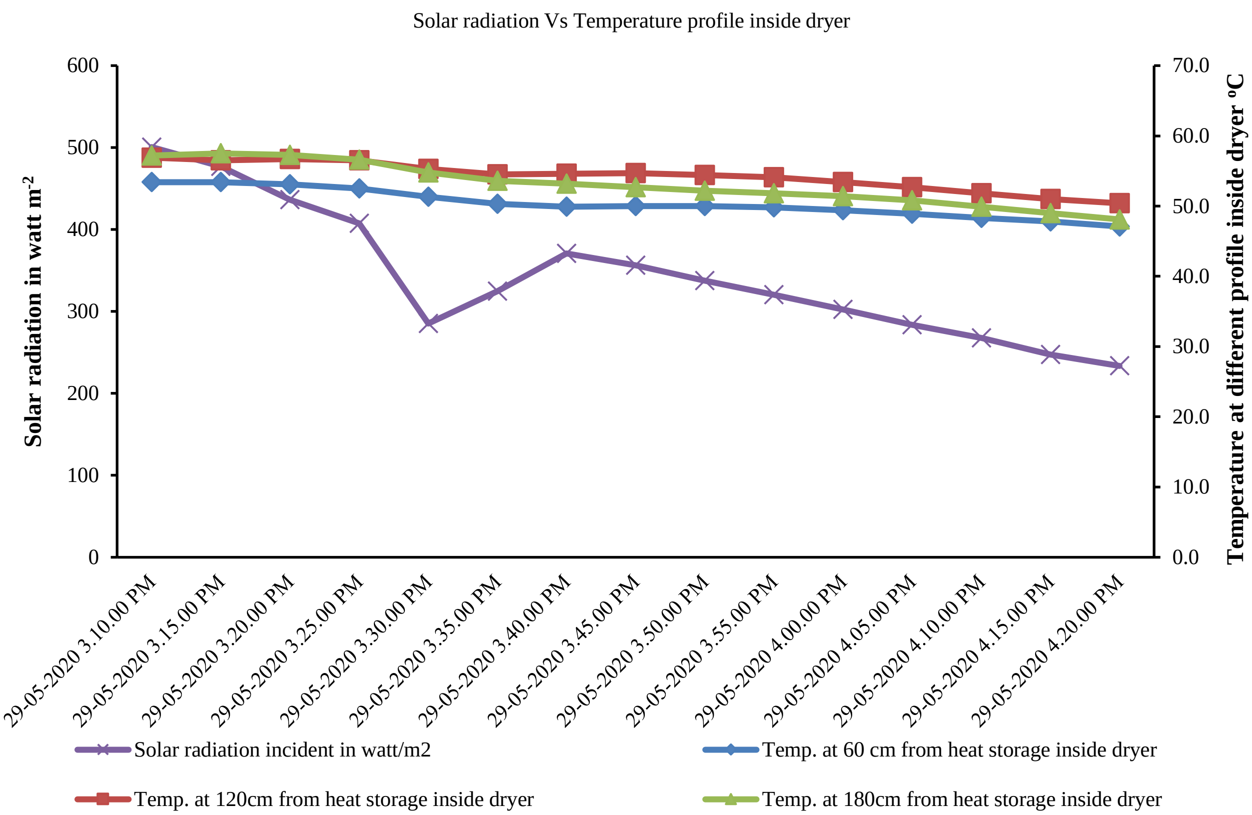

Figure 16 Marginal lowering of temperature profiles corresponding to significant reduction of solar radiation in afternoon hours

3.2.2 Test result of improvised air inlets with flat plate collectors

As shown in Figure 15, flat plate collectors were installed at the air inlets to increase the initial air temperature of the dryer during the active drying period in daylight hours. A comparative illustration of the dryer in operation is presented with and without a flat plate collector. Observations recorded exhibit a decrease in the relative humidity of incoming air from 38.5% to 40% and an increase in temperature from 25% to 28% relative to ambient levels, respectively, as shown in Figure17.

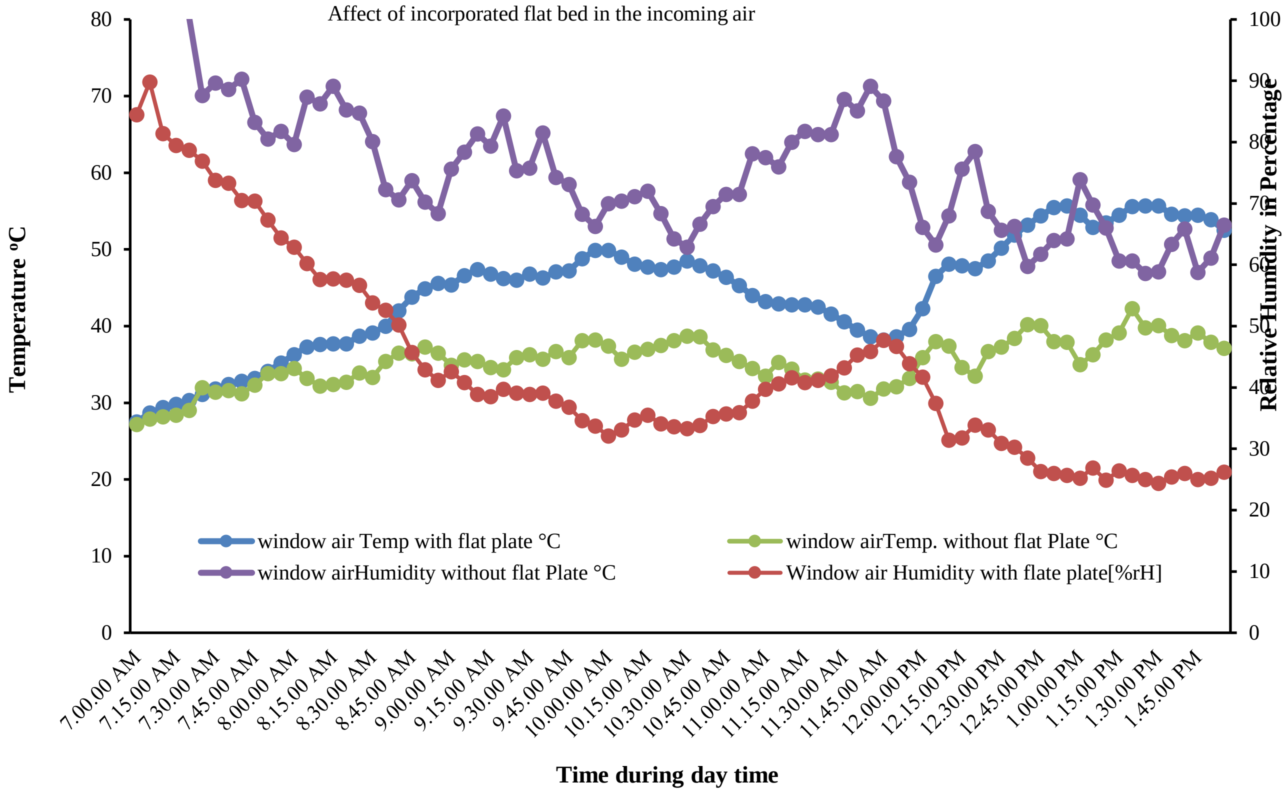

Figure 17 Comparison of temperatures and humidity with and without flat plate collectors at air inlets under no-load testing

3.2.3 Transition from natural to forced convection mode and its essentiality

The airflow inside the dryer under natural convection ranges from 0.4 m sec^{-1} in the morning to 0.9 m sec^{-1} at noon. Under forced convection, the average air flow velocity inside the dryer is from 1.4 to 1.6 m sec^{-1}. Low airflow rates are more energy-efficient, utilizing thermal energy effectively. From an energy perspective, a low airflow rate is advantageous in drying operations, as it employs a greater proportion of thermal energy compared to higher airflow rates (Boughali et al., 2009).

The drying process in a solar tunnel dryer requires materials to remain inside for longer periods, especially overnight, to complete the drying process, increasing the risk of spoilage. To counter this, forced convection is implemented with a continuously operating fan at night, controlled by humidity sensors - the fan activates above 60% humidity and deactivates below 50%.

From the viewpoint of relative humidity, drying conditions at 40% relative humidity produce better color and aroma than those at 20% or 60% humidity. As per Xu et al. (2021), samples dried under relative humidity levels of 20%, 40%, and 60% indicated that 40% humidity in hot air produced the best color and aroma.

A challenge with greenhouse dryers is condensation from saturated air, especially in cooler, high-humidity conditions (around 90% humidity) during early mornings, where the dew point is approximately 1.4 to 1.6 degrees Celsius below the ambient temperature. Increased air velocity through forced convection helps minimize dew formation.

3.3 Testing of the greenhouse dryer under loaded conditions

The greenhouse dryer is used for drying 650 kg of turmeric in one batch over a period of three and a half days. Experiments on drying freshly harvested turmeric were conducted using both open sun drying (OSD) and thermal energy-stored greenhouse drying (GHD). After routine blanching, 650 kg of fresh turmeric was loaded into the dryer at 11:20 AM on February 18, 2021 (Figure 18). Figure 19) illustrates data on solar radiation (watts per square meter), average air temperature, and relative humidity within GHD and the surrounding environment from February 18 to February 21, 2021. February 18th and 21st were sunny, while February 19th and 20th were slightly cloudy. Forced convection mode starts when the dryer's relative humidity exceeds 60%. On the 18th, 19th, and 20th, between 8:50 PM and 4:50 AM in next day, the dryer’s humidity is lower than the ambient humidity, yet its internal temperature surpasses the ambient temperature. The thermal energy storage of the concrete foundation of the GHD mitigates the variations in solar radiation caused by cloud cover on the second and third drying days; as demonstrated in Figure 19, there is negligible change in the internal temperature and relative humidity of the dryer.

Figure 18 View of the GHD under loaded condition of turmeric

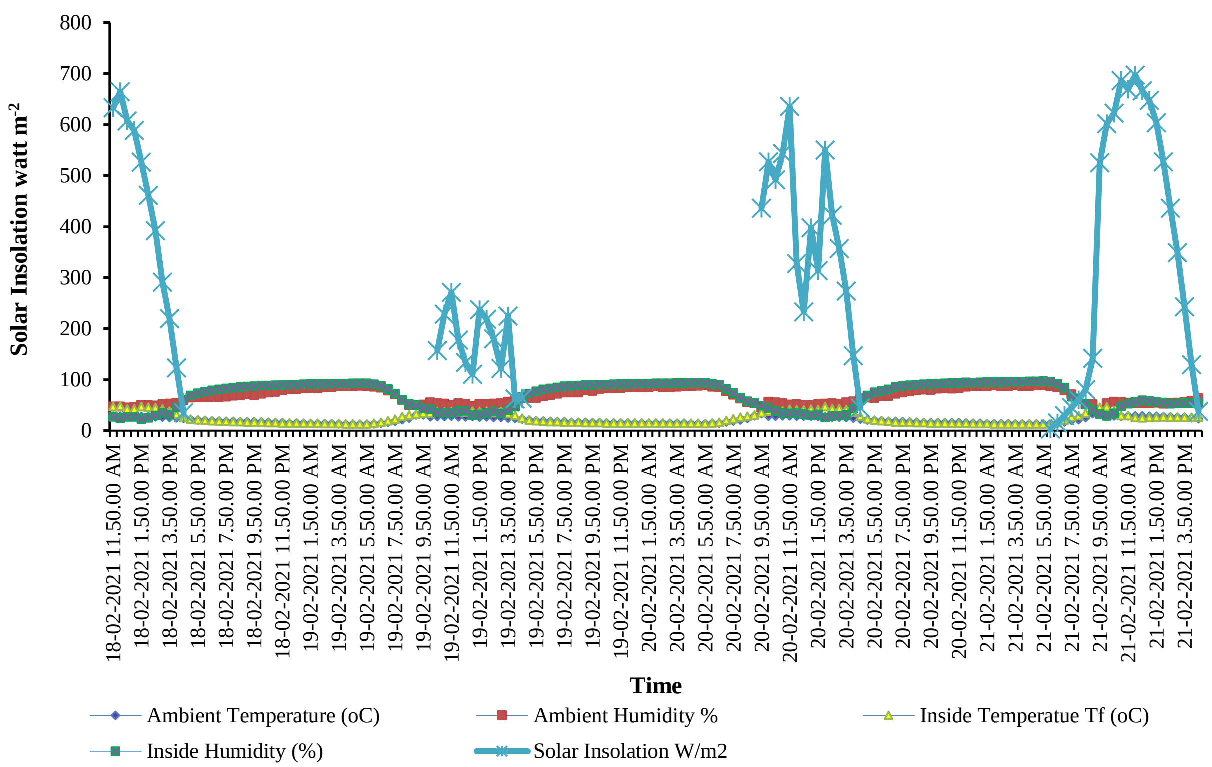

Figure 19 Turmeric drying experiment, data on solar radiation, average air temperature, and the relative humidity within the GSD and the ambient

3.3.2 Comparing turmeric drying in GHD and open solar drying

The drying characteristics of turmeric slices were examined under Open Sun Drying (OSD) and Greenhouse Drying (GHD), as illustrated in Figure 20. GHD demonstrated a superior moisture extraction rate relative to OSD. In GHD, the moisture content of sliced turmeric diminished from 585.87% (db) to 13.43% (db) over a period of 22 hours. Conversely, the moisture content of sliced turmeric decreased to 91.13% (db) after the exact duration of open solar drying. The thermal efficiency of the greenhouse dryer, calculated using Equation 2, was determined to be 28.89%.

While plotting the moisture ratio against drying time, it was observed that the drying rate under GHD was much faster in the initial hours of drying. However, it became extremely low after 11-12 hours of drying, as shown in Figure 21.

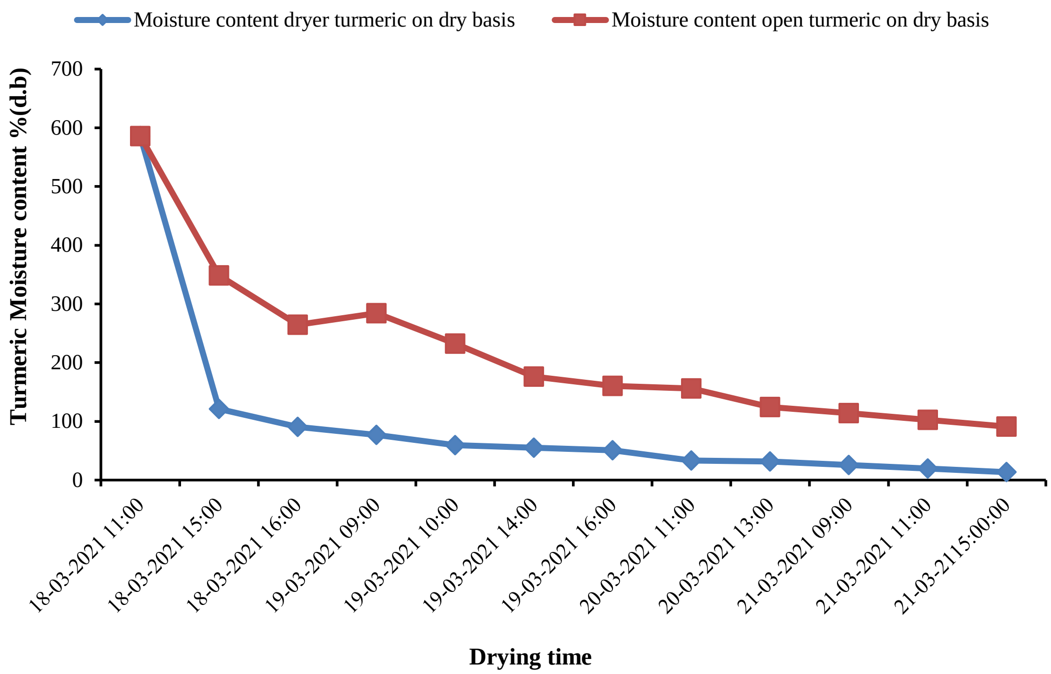

Figure 20 Comparison of slice turmeric drying between GHD and OSD

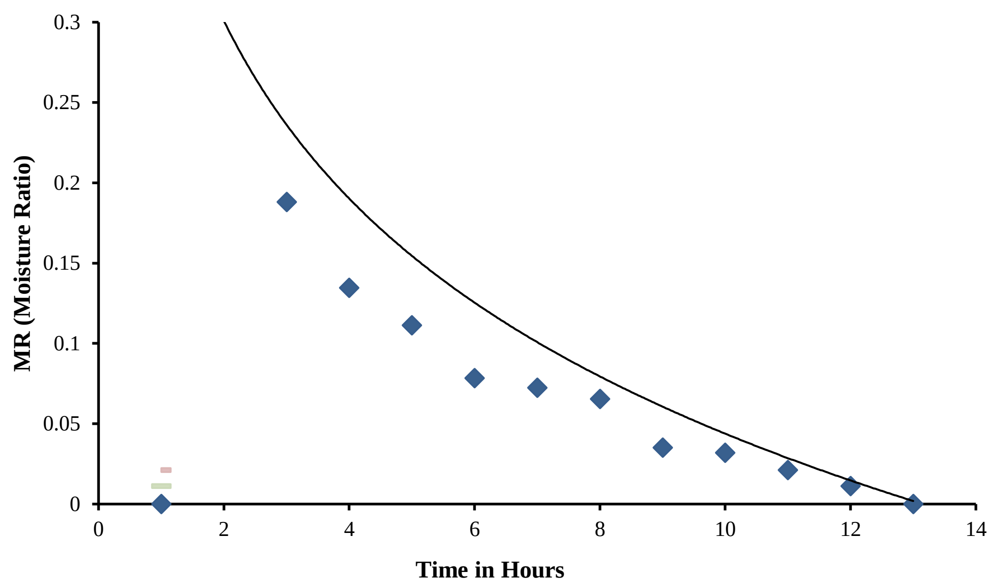

Figure 21 Moisture ratios against drying time

Effective moisture diffusivity of turmeric drying in GHD is obtained from Equation 4 by calculating the slopes derived from the linear regression of $ln (MR) = ln A - kt$ versus time data. GHD is tested against thin-layer drying mathematical models with the help of the moisture ratio (MR) calculated by Equation 3. The drying behavior of thin-layer drying of turmeric in GHD is tested against four models, namely Page, Modified Page, Henderson and Hang, and Singh model. Among the four models, the Page model resulted in the highest R^2 (0.9946) and the lowest values of SEE (0.0200). As such, Page model may be assumed to represent the thin layer drying behaviour of sliced turmeric in GHD.

3.3.3 Quality attributes of fresh and dry turmeric

In the dried sample of turmeric, beta-tumeron was reduced by 15.34% with respect to the fresh sample, as compared to the GC-MS analysis reports of fresh and dried extracts of Turmeric.

3.3.4 Cost analysis of Heat storage based GHD

The price of the heat storage-based greenhouse dryer is INR 1 20,000 according to the market rate in Jorhat, Assam, India. Drying nine batches of turmeric in a single harvesting season is feasible. Considering the cost of fresh turmeric fingerling as INR 25 per kg and dried turmeric as INR 220 per kg, the payback period for drying turmeric solely, accounting for all variable and fixed costs, is determined to be two and a half years. Using another dried product, such as ginger or elephant apple, will further decrease the payback period.

4 Conclusion

Most of the researched solar dryers have capacities of 100 and 500 kg in a batch. So development and evaluation of a natural convection-based dryer of capacity 50 kg to 1000 kg is taken up in this study. As per earlier researchers, the dryer structure is standardized from segmented dimensions (width, length, and height) to a perfectly hemi-cylindrical form (10.2 m span, 2 m radius). To retain heat, the north and east walls of the heat storage basement are insulated with polystyrene, and the South and western sides are painted black. Air flow is maintained by the dryer's southern base air inlets and natural buoyant draft through the chimney at the top. For cost-effective automation, humidity sensor-based forced convection expedites evacuating hot, humid out-flowing air. Overcoming double container airflow velocity results in turbulence. (0.4–0.9 to 1.4–1.6 m s^{-1}). This improved airflow prevents any dew formation.

Enhanced air circulation avoids any condensation from dripping into the dryer. The greenhouse dryer's air temperature is 9°C -18°C higher than the outdoors on sunny days during no-load testing and 4°C -10°C higher on partially overcast days during active drying hours. The sensor activates the forced convection system when the dryer's relative humidity is over 60% and deactivates it below 40%.

Temperature and relative humidity were monitored throughout drying. Flat plate collectors at the intake raised the dryer's starting air temperature and reduced air humidity by 25%–28% and 38.5%–40%, respectively, during daylight hours. Under loaded conditions, 940 kg of full-blanched turmeric fingerlings and rhizomes with an average moisture content of 87.38% dry to 10.71% in 62–80 hours. Blanched turmeric slices can be dried in 26–36 hours. At 521.46 watts per square meter solar radiation, the GSD had 28.89% thermal efficiency. The dryer costs INR 1,20,000, and the annual payback period for drying turmeric in nine batches is 2.5 years.

Acknowledgement

The authors are grateful to Assam Agricultural University to facilitate the fabrication and commissioning of the dryer at Instructional cum Research Farm at Assam Agricultural University, Jorhat.

Conflict of Interest

The author(s) declare no conflict of interest.

Authors' Contribution

Manas Jyoti Barooah analyzed data, participated in determining the experimental design, engineered plants, performed stress experiments, created figures, and drafted the manuscript. Laxmi Narayan Sethi helped in conceiving the study. Abhijit Borah participated in designing the study. Aradhana Boruah contributed to the text and content of the manuscript. Ajita Tiwari participated in data interpretation and drafted the manuscript text and the content of the manuscript, including revisions and edits.

Data Availability Statement

The manuscript incorporates all datasets produced or examined throughout this research study.

Ethics Statement

The document accurately and thoroughly presents the authors' original research and analysis.

Reference

ACI Committee 302. 2004. Guide for concrete floor and slab construction reported by ACI Committee 302. ACI 302.1R-04, 1-77. Retrieved from https://www.studocu.com/latam/document/universidad-centroamericana/diseno-de-elementos-de-concreto-reforzado-ii/aci-302-1r-04-pisos-industriales/43824304. Accessed 22/04/2020

Ahmad, A., and O. Prakash. 2020. Performance evaluation of a solar greenhouse dryer at different bed conditions under passive mode. *Journal of Solar Energy Engineering*, 142(1): 011006.

Ahmad, A., O. Prakash, S. K. Sarangi, P. S. Chauhan, R. Chatterjee, S. Sharma, R. Kumar, S. M. Tag, A. Kumar, B. Salah, and S. S. Ullah. 2023. Thermal and CFD analyses of sustainable heat storage-based passive greenhouse dryer operating in no-load condition. *Sustainability*, 15(15): 12067.

Ambesange, A. I., and S. K. Kusekar. 2017. Analysis of flow through solar dryer duct using CFD. *International Journal of Engineering Development and Research*, 5(1): 534-552.

Ayyappan, S., and K. Mayilsamy. 2012. Solar tunnel drier with thermal storage for drying of copra. *International Journal of Energy Technology and Policy*, 8(1): 3-13.

Ayyappan, S., K. Mayilsamy, and V. V. Sreenarayanan. 2015. Performance improvement studies in a solar greenhouse drier using sensible heat storage materials. *Heat and Mass Transfer*, 52(3): 459-467.

Berroug, F., E. K. Lakhal, M. El Omari, M. Faraji, and H. El Qarnia. 2011. Thermal performance of a greenhouse with a phase change material north wall. *Energy and Buildings*, 43(11): 3027-3035.

Boughali, S., H. Benmoussa, B. Bouchekima, D. Mennouche, H. Bouguettaia, and D. Bechki. 2009. Crop drying by indirect active hybrid solar - Electrical dryer in the eastern Algerian Septentrional Sahara. *Solar Energy*, 83(12): 2223-2232.

Das, D., M. Roy, and T. Basak. 2016. Studies on natural convection within enclosures of various (non-square) shapes – A review. *International Journal of Heat and Mass Transfer*, 106: 356-406.

Dikshit, K. R., and J. K. Dikshit. 2014. *North-East India: Land, People and Economy.* Netherlands: Springer.

Ekechukwu, O. V., and B. Norton, 1999. Review of solar-energy drying systems II: An overview of solar drying technology. *Energy Conversion and Management*, 40(3): 615-655.

Ekechukwu, O. V., and B. Norton. 1997. Experimental studies of integral-type solar-energy tropical crop dryers. *Energy Conversion and Management*, 38(14): 1483-1500.

Geankoplis, C. J. 2016. *Transport processes and separation process principles (includes unit operations)* (4th ed.). Boston, USA: Pearson Education.

Gholamalizadeh, E., and M. H. Kim. 2014. Three-dimensional CFD analysis for simulating the greenhouse effect in solar chimney power plants using a two-band radiation model. *Renewable Energy*, 63: 498-506.

Hii, C. L., R. A. Rahman, S. Jinap, and Y. B. Che Man. 2006. Quality of cocoa beans dried using a direct solar dryer at different loadings. *Journal of the Science of Food and Agriculture*, 86(8): 1237-1243.

Rathore, N. S., and N. L. Panwar. 2010. Design and development of energy efficient solar tunnel dryer for industrial drying. *Clean Technologies and Environmental Policy*, 13(1): 125-132.

Ratti, C., and A. S. Mujumdar. 1997. Solar drying of foods:

Modeling and numerical simulation. *Solar Energy*, 60(3-4): 151-157.

Seveda, M. S. 2012. Design and development of walk-in type hemicylindrical solar tunnel dryer for industrial use. *International Scholarly Research Notices*, 2012: 890820.

Velić, D., M. Planinić, S. Tomas, and M. Bilić. 2004. Influence of airflow velocity on kinetics of convection apple drying. *Journal of Food Engineering*, 64(1): 97-102. (Couldn't be found in the main body)

Xu, W., M. N. Islam, X. Cao, J. Tian, and G. Zhu. 2021. Effect of relative humidity on drying characteristics of microwave-assisted hot air drying and qualities of dried finger citron slices. *LWT - Food Science and Technology*, 137: 110413.